Recursive T-Matrix Algorithms for the Solution of Electromagnetic Scattering from Strip and Patch Geometries

Levent Gürel, *Member, IEEE,* and Weng Cho Chew, *Fellow, IEEE*

***Abstract*— Two recursive T-matrix algorithms (RTMA's) are presented and their reduced computational complexities and reduced memory requirements are demonstrated. These algorithms are applied to the problem of electromagnetic scattering from conducting strip and patch geometries. For a systematic development, canonical geometries of strips and patches are chosen. These geometries are reminiscent of finite-sized frequency selective surfaces (FSS's). Computational complexities of $O(N^2)$ and $O(N^{7/3})$ and memory requirements of $O(N)$ and $O(N^{4/3})$ are shown to be feasible for two-dimensional and three-dimensional geometries, respectively. The formulation uses only two components of the electric field. Therefore, the vector electromagnetic problem of scattering from three-dimensional patch geometries can be solved using scalar—rather than vector—addition theorems for spherical harmonic wave functions. For a two-dimensional strip problem, both TM and TE polarizations can be solved simultaneously using this formulation. Numerical scattering results are presented in the form of radar cross sections (RCS's) and validated by comparison with the method of moments (MoM).**

I. Introduction

Two efficient and fast algorithms for the numerical solution of the integral-equation formulations of the electromagnetic scattering problems will be presented in this paper. These are the recursive T-matrix algorithm (RTMA) and the recursive aggregate T-matrix algorithm (RATMA), which will be collectively referred to as the recursive T-matrix algorithms (RTMA's) [1]–[12]. The RTMA's will be applied to canonical representatives of a class of geometries that contain conducting strips and patches.

Several important classes of problems in computational electromagnetics (including those that are of interest in this paper) can be formulated using integral equations (IE) and solved by matrix solvers, e.g., Gaussian elimination, after converting the integral equations to matrix equations, e.g., via method of moments (MoM). Such a solution scheme (henceforth referred to as IE-MoM) is powerful and general since

1) it is flexible, and it can easily be formulated and implemented,
2) it is valid for all excitations or incident waves (multiple "right-hand sides"),
3) it is also applicable to eigenvalue problems, and
4) it incorporates the radiation condition and, therefore, can handle geometries radiating or scattering into unbounded regions as well as geometries in bounded regions.

A problem comprising N unknowns requires $O(N^3)$ operations and $O(N^2)$ memory locations with this type of a solution. Other formulation schemes (e.g., the finite-element method) and solution techniques (e.g., the conjugate-gradient algorithm) with lower computational complexities and memory requirements are possible, but they are not as general as the integral-equation formulation outlined above.

Despite all of the advantages of IE-MoM, its $O(N^3)$ computational complexity and $O(N^2)$ memory requirement exhaust computational resources before larger and more interesting problems can be solved. A general solution scheme with reduced computational complexity and memory requirement is essential for problems comprising very large numbers of unknowns [33]–[41].

As a partial solution to the computational-complexity and the memory-requirement problems referred to above, two recursive T-matrix algorithms will be presented in this paper. It will be shown that these algorithms have less than $O(N^3)$ computational complexities and less than $O(N^2)$ memory requirements for some classes of geometries.

II. Canonical Geometries

Canonical geometries of strips and patches are shown in Figs. 1 and 2. Illustrated in parts (a) and (b) of Fig. 1 are the one-dimensional and two-dimensional clusterings of strips. Similarly, (a) and (b) of Fig. 2 display the two-dimensional and three-dimensional clusterings of patches. In this paper, we will apply the RTMA's to these geometries. Canonical problems are important since they display the performances of the solution techniques on the class of geometries they are representing, without having to apply the solution technique under test to each member geometry of the class. The canonical problems illustrated in Figs. 1 and 2 are also important on their

Manuscript received April 23, 1992; revised August 24, 1992. This work was supported by the National Science Foundation under grant NSF ECS-85-25981, and the Office of Naval Research under grant N000-14-89-J-1286, with matching funds from Northrop and General Electric.

L. Gürel is with the IBM Research Division, T.J. Watson Research Center, Yorktown Heights, NY 10591. He was formerly with the Electromagnetics Laboratory, Department of Electrical and Computer Engineering, University of Illinois, Urbana, IL 61801.

W. C. Chew is with the Electromagnetics Laboratory, Department of Electrical and Computer Engineering, University of Illinois, Urbana, IL 61801.

IEEE Log Number 9205474

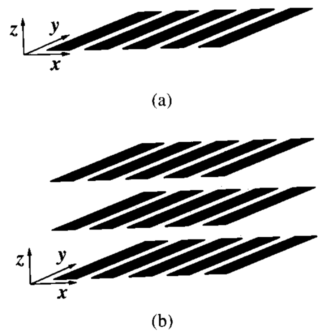

Fig. 1. Canonical problems for strips: **(a)** one-dimensional clustering of strips; **(b)** two-dimensional clustering of strips.

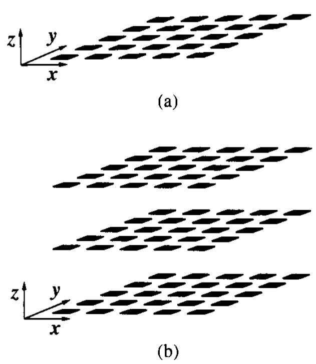

Fig. 2. Canonical problems for patches: **(a)** two-dimensional clustering of patches; **(b)** three-dimensional clustering of patches.

own account since they or a slight modification thereof can be considered as finite-size frequency-selective surfaces.

III. Algorithms

The x and y components of the electric field will be used to represent the electromagnetic fields. For a two-dimensional strip problem, the x and y components represent the TE (to y) and TM (to y) cases, respectively. Following the standard T-matrix notation [14]–[32],[1]–[12], the incident field can be expressed as

$$\mathbf{E}_t^I(\mathbf{r}) = \begin{bmatrix} E_x^I(\mathbf{r}) \\ E_y^I(\mathbf{r}) \end{bmatrix} = \begin{bmatrix} \Re g\boldsymbol{\psi}_x^t(\mathbf{r}) & 0 \\ 0 & \Re g\boldsymbol{\psi}_y^t(\mathbf{r}) \end{bmatrix} \cdot \begin{bmatrix} \mathbf{e}_x \\ \mathbf{e}_y \end{bmatrix} = \Re g\overline{\boldsymbol{\Psi}}^t(\mathbf{r}) \cdot \mathbf{e} \tag{1}$$

and the scattered field as

$$\mathbf{E}_t^S(\mathbf{r}) = \begin{bmatrix} E_x^S(\mathbf{r}) \\ E_y^S(\mathbf{r}) \end{bmatrix} = \sum_{i=1}^{N} \begin{bmatrix} \boldsymbol{\psi}_x^t(\mathbf{r}_i) & 0 \\ 0 & \boldsymbol{\psi}_y^t(\mathbf{r}_i) \end{bmatrix} \cdot \begin{bmatrix} \mathbf{f}_{xi} \\ \mathbf{f}_{yi} \end{bmatrix} = \sum_{i=1}^{N} \overline{\boldsymbol{\Psi}}^t(\mathbf{r}_i) \cdot \mathbf{f}_i \tag{2}$$

where $\boldsymbol{\psi}(\mathbf{r})$ is a column vector containing outgoing scalar spherical (cylindrical) harmonic wave functions in a three-dimensional (two-dimensional) patch (strip) problem and $\Re g\boldsymbol{\psi}(\mathbf{r})$ is the "regular part" of $\boldsymbol{\psi}(\mathbf{r})$, i.e., $\Re g\boldsymbol{\psi}(\mathbf{r})$ contains standing harmonic wave functions[1].

T matrices, which relate the scattered-field coefficients to the incident-field coefficients, are defined for each scatterer via the relation

$$\boldsymbol{f}_i = \begin{bmatrix} \boldsymbol{f}_{xi} \\ \boldsymbol{f}_{yi} \end{bmatrix} = \begin{bmatrix} \overline{\mathbf{T}}_{i(N)}^{xx} & \overline{\mathbf{T}}_{i(N)}^{xy} \\ \overline{\mathbf{T}}_{i(N)}^{yx} & \overline{\mathbf{T}}_{i(N)}^{yy} \end{bmatrix} \cdot \begin{bmatrix} \overline{\boldsymbol{\beta}}_{i0}^x & 0 \\ 0 & \overline{\boldsymbol{\beta}}_{i0}^y \end{bmatrix} \cdot \begin{bmatrix} \mathbf{e}_x \\ \mathbf{e}_y \end{bmatrix} = \overline{\mathbf{T}}_{i(N)} \cdot \overline{\boldsymbol{\beta}}_{i0} \cdot \mathbf{e} \tag{3}$$

so that the scattered field can be expressed in terms of these T matrices, i.e.,

$$\mathbf{E}_t^S(\mathbf{r}) = \sum_{i=1}^{N} \overline{\boldsymbol{\Psi}}^t(\mathbf{r}_i) \cdot \overline{\mathbf{T}}_{i(N)} \cdot \overline{\boldsymbol{\beta}}_{i0} \cdot \mathbf{e}\,. \tag{4}$$

In the above, one T matrix is defined for each scatterer, i.e., the subscript i denotes the ith scatterer. The parenthesized N in the subscript is an "environment parameter," which denotes the presence of N scatterers in the geometry when $\overline{\mathbf{T}}_{i(N)}$ is defined. The translation matrices $\overline{\boldsymbol{\beta}}_{ij}$ (and $\overline{\boldsymbol{\alpha}}_{ij}$) [1]–[13] are obtained using scalar addition theorems for either spherical or cylindrical harmonic wave functions. This formulation enables one to avoid the more cumbersome vector addition theorems for the three-dimensional patch problems and to use the considerably fast recurrence-relation computation of the three-dimensional scalar addition theorem [13].

In the presence of N scatterers (or subscatterers), the T matrices $\overline{\mathbf{T}}_{i(N)} \cdot \overline{\boldsymbol{\beta}}_{i0}$ for $i = 1, \cdots, N$ can be computed from the $(N-1)$-scatterer T matrices ($\overline{\mathbf{T}}_{i(N-1)} \cdot \overline{\boldsymbol{\beta}}_{i0}$, $i = 1, \cdots, N-1$) using the recursive relations [3],[5]

$$\overline{\mathbf{T}}_{N(N)} \cdot \overline{\boldsymbol{\beta}}_{N0} = \left(\overline{\mathbf{I}} - \overline{\mathbf{T}}_{N(1)} \cdot \sum_{i=1}^{N-1} \overline{\boldsymbol{\alpha}}_{Ni} \cdot \overline{\mathbf{T}}_{i(N-1)} \cdot \overline{\boldsymbol{\beta}}_{i0} \cdot \overline{\boldsymbol{\alpha}}_{0N} \right)^{-1} \cdot \overline{\mathbf{T}}_{N(1)} \cdot \left(\overline{\boldsymbol{\beta}}_{N0} + \sum_{m=1}^{N-1} \overline{\boldsymbol{\alpha}}_{Nm} \cdot \overline{\mathbf{T}}_{m(N-1)} \cdot \overline{\boldsymbol{\beta}}_{m0} \right). \tag{5}$$

$$\overline{\mathbf{T}}_{i(N)} \cdot \overline{\boldsymbol{\beta}}_{i0} = \overline{\mathbf{T}}_{i(N-1)} \cdot \overline{\boldsymbol{\beta}}_{i0} + \overline{\mathbf{T}}_{i(N-1)} \cdot \overline{\boldsymbol{\beta}}_{i0} \cdot \overline{\boldsymbol{\alpha}}_{0N} \cdot \overline{\mathbf{T}}_{N(N)} \cdot \overline{\boldsymbol{\beta}}_{N0} \quad \text{for } i = 1, 2, \cdots, N-1\,. \tag{6}$$

Equations (5) and (6) together constitute the *recursive T-matrix algorithm (RTMA).*

By using the definition of the *aggregate T matrix* [4],[5]

$$\overline{\boldsymbol{\tau}}_{(N)} = \sum_{i=1}^{N} \overline{\boldsymbol{\beta}}_{0i} \cdot \overline{\mathbf{T}}_{i(N)} \cdot \overline{\boldsymbol{\beta}}_{i0} \tag{7}$$

in (5) and (6), one can convert the RTMA to another recursive algorithm to compute the N-scatterer aggregate T matrix, $\overline{\boldsymbol{\tau}}_{(N)}$, from the $(N-1)$-scatterer aggregate T matrix, $\overline{\boldsymbol{\tau}}_{(N-1)}$. This algorithm is called the *recursive aggregate-T-matrix*

[1]Explicit expressions for the $\boldsymbol{\psi}(\mathbf{r})$ and $\Re g\boldsymbol{\psi}(\mathbf{r})$ vectors are given elsewhere [12].

algorithm (RATMA) and is given by

$$\overline{\mathbf{T}}_{N(N)} \cdot \overline{\boldsymbol{\beta}}_{N0} = \left(\overline{\mathbf{I}} - \overline{\mathbf{T}}_{N(1)} \cdot \overline{\boldsymbol{\alpha}}_{N0} \cdot \overline{\boldsymbol{\tau}}_{(N-1)} \cdot \overline{\boldsymbol{\alpha}}_{0N}\right)^{-1} \cdot \overline{\mathbf{T}}_{N(1)} \cdot \left(\overline{\boldsymbol{\beta}}_{N0} + \overline{\boldsymbol{\alpha}}_{N0} \cdot \overline{\boldsymbol{\tau}}_{(N-1)}\right) \quad (8)$$

$$\overline{\boldsymbol{\tau}}_{(N)} = \overline{\boldsymbol{\tau}}_{(N-1)} + \overline{\boldsymbol{\beta}}_{0N} \cdot \overline{\mathbf{T}}_{N(N)} \cdot \overline{\boldsymbol{\beta}}_{N0} + \overline{\boldsymbol{\tau}}_{(N-1)} \cdot \overline{\boldsymbol{\alpha}}_{0N} \cdot \overline{\mathbf{T}}_{N(N)} \cdot \overline{\boldsymbol{\beta}}_{N0}. \quad (9)$$

For brevity, we have not included the derivations of the RTMA's here. A variety derivations can be found elsewhere [1]–[10],[12].

IV. Computational Complexities and Memory Requirements

As shown earlier [1]–[12], the addition theorems, which involve infinite summations in principle, can be truncated to P terms within a specified error ϵ. There exists a P for every ϵ and P increases as ϵ decreases. Furthermore, if one keeps M terms in the multipole expansion of (2), then the sizes of the T matrices, $\overline{\mathbf{T}}_{i(N)} \cdot \overline{\boldsymbol{\beta}}_{i0}$, become $M \times P$. Similarly, the sizes of the aggregate T matrices, $\overline{\boldsymbol{\tau}}_{(N)}$, are $P \times P$.

At an intermediate step of the RTMA, the n-scatterer T matrices can be computed from the knowledge of the $(n-1)$-scatterer T matrices by going once through (5) and (6). By counting the number of operations required to do this, it is observed that the computational complexity of this single step is $O(M^3 + nM^2P)$. For an N-scatterer problem, this step has to be repeated N times. Then, the computational complexity of the whole algorithm is found to be $O(NM^3 + N^2M^2P)$, where N is the total number of unknowns in the problem, M is the number of harmonics used to expand the scattered field of each scatterer, and P is the number of terms kept in the truncated addition theorems that are used to translate the coordinate system of one scatterer to that of another. M, which depends only on the size of the subscatterers, can be kept constant at a value that satisfies the convergence criteria for every scatterer in the problem. Then, the computational complexity of the T-matrix algorithm can be expressed as $O(N^2P)$.

Similarly, the number of operations required at the nth step of the RATMA given by (8) and (9) is $O(M^3 + MP^2)$. For an N-scatterer problem, the RATMA has the overall complexity $O(NM^3 + NMP^2)$. Again, M can be kept constant throughout the problem, and the expression for the computational complexity reduces to $O(NP^2)$.

In the RTMA solution of an N-scatterer problem, one needs to store N number of T matrices of size $M \times P$. Thus, the memory requirement of the RTMA is $O(NP)$. On the other hand, the dominant memory requirement in the RATMA is due to a single $P \times P$ aggregate T matrix. Thus, the memory requirement of the RATMA is $O(P^2)$.

Finding the dependence of P on N is imperative for evaluating the performance of the RTMA's. From a simple argument, it follows that the number of terms in the addition theorems, P, asymptotically becomes linearly dependent on the magnitudes of the arguments of the Bessel functions [7].

TABLE I
Computational Compexities and Memory Requirements of the RTMA's for Different Clusterings of Two-Dimensional Scatterers

Dimension of Clustering	Algorithm	
	RTMA	RATMA
(a) Computational Complexity		
Generic Computational Complexity	$O(N^2P)$	$O(NP^2)$
One-Dimensional Clustering ($P \propto N$)	$O(N^3)$	$O(N^3)$
Two-Dimensional Clustering ($P \propto N^{1/2}$)	$O(N^{5/2})$	$O(N^2)$
(b) Memory Requirement		
Generic Memory Requirement	$O(NP)$	$O(P^2)$
One-Dimensional Clustering ($P \propto N$)	$O(N^2)$	$O(N^2)$
Two-Dimensional Clustering ($P \propto N^{1/2}$)	$O(N^{3/2})$	$O(N)$

TABLE II
Computational Complexities and Memory Requirements of the RTMA's for Different Clusterings of Three-Dimensional Scatterers

Dimension of Clustering	Algorithm	
	RTMA	RATMA
(a) Computational Complexity		
Generic Computational Complexity	$O(N^2P)$	$O(NP^2)$
Two-Dimensional Clustering ($P \propto N$)	$O(N^3)$	$O(N^3)$
Three-Dimensional Clustering ($P \propto N^{2/3}$)	$O(N^{8/3})$	$O(N^{7/3})$
(b) Memory Requirement		
Generic Memory Requirement	$O(NP)$	$O(P^2)$
Two-Dimensional Clustering ($P \propto N$)	$O(N^2)$	$O(N^2)$
Three-Dimensional Clustering ($P \propto N^{2/3}$)	$O(N^{5/3})$	$O(N^{4/3})$

Since the largest magnitude of the arguments, $d_{\max}$, is the largest dimension of the geometry under consideration, we arrive at

$$P \propto d_{\max}^{\alpha}, \quad \alpha \leq 1 \text{ for cylindrical harmonics} \quad (10a)$$

$$\sqrt{P} \propto d_{\max}^{\alpha}, \quad \alpha \leq 1 \text{ for spherical harmonics}. \quad (10b)$$

For large values of $d_{\max}$ and P, it is found that α approaches unity. In the rest of the analysis, assuming that the worst case holds, one can safely let

$$\alpha = 1. \quad (10c)$$

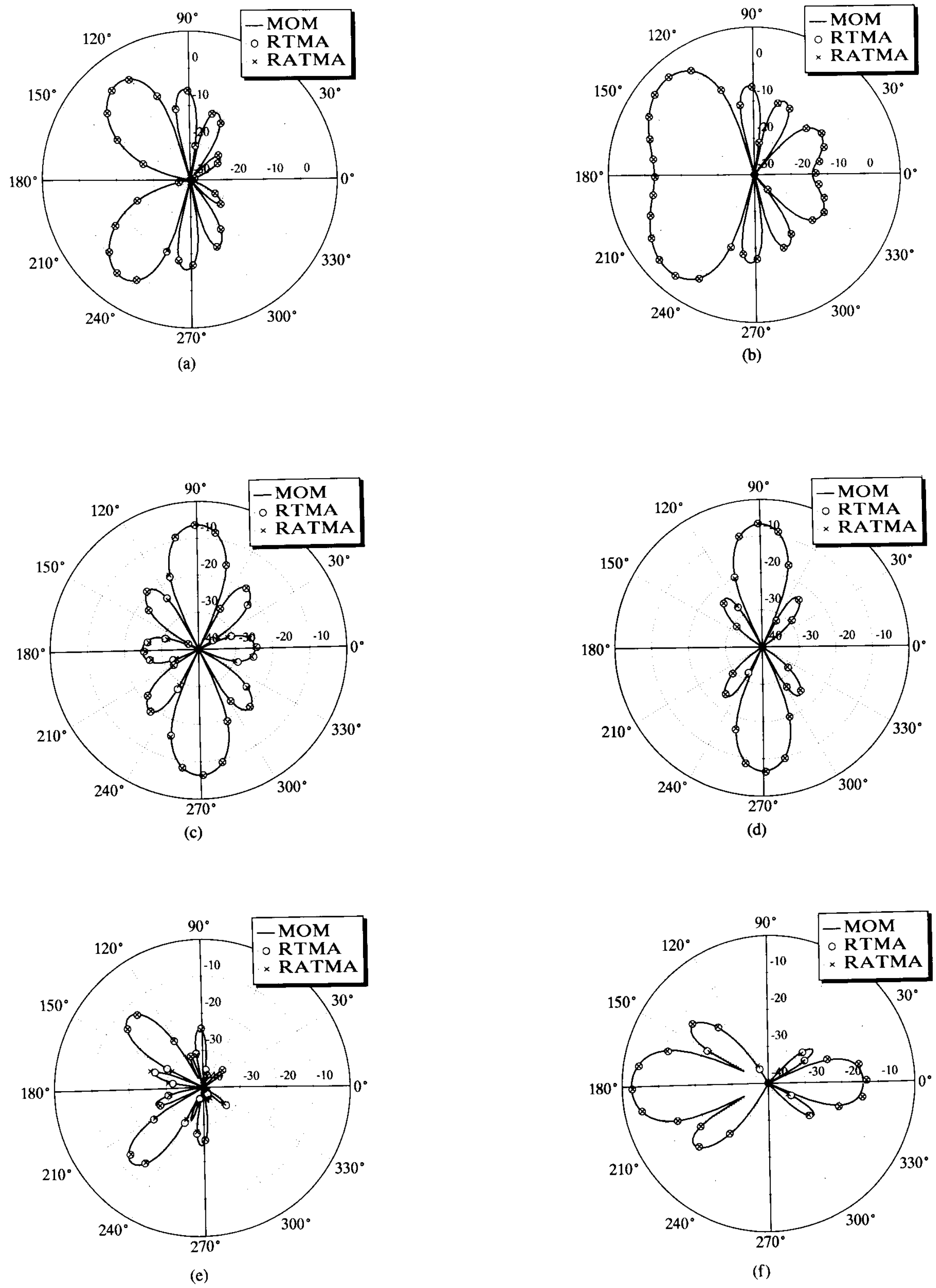

Fig. 3. RCS plots due to the 7 × 7 array configuration of two-dimensional clustering of patches as in Fig. 2(a): **(a)** TE case on the $\phi = 0$ cut, **(b)** TE case on the $\phi = \frac{\pi}{2}$ cut, **(c)** TE case on the $\theta = \frac{\pi}{2}$ cut, **(d)** TM case on the $\phi = 0$ cut, **(e)** TM case on the $\phi = \frac{\pi}{2}$ cut, **(f)** TM case on the $\theta = \frac{\pi}{2}$ cut.

For different clusterings of the scatterers, $d_{\max}$ has a different dependence on N. We will investigate the types of clusterings illustrated in Figs. 1 and 2, namely,

1) one-dimensional clustering of two-dimensional scatterers [Fig. 1(a)],
2) two-dimensional clustering of two-dimensional scatterers [Fig. 1(b)],
3) two-dimensional clustering of three-dimensional scatterers [Fig. 2(a)],
4) three-dimensional clustering of three-dimensional scat-

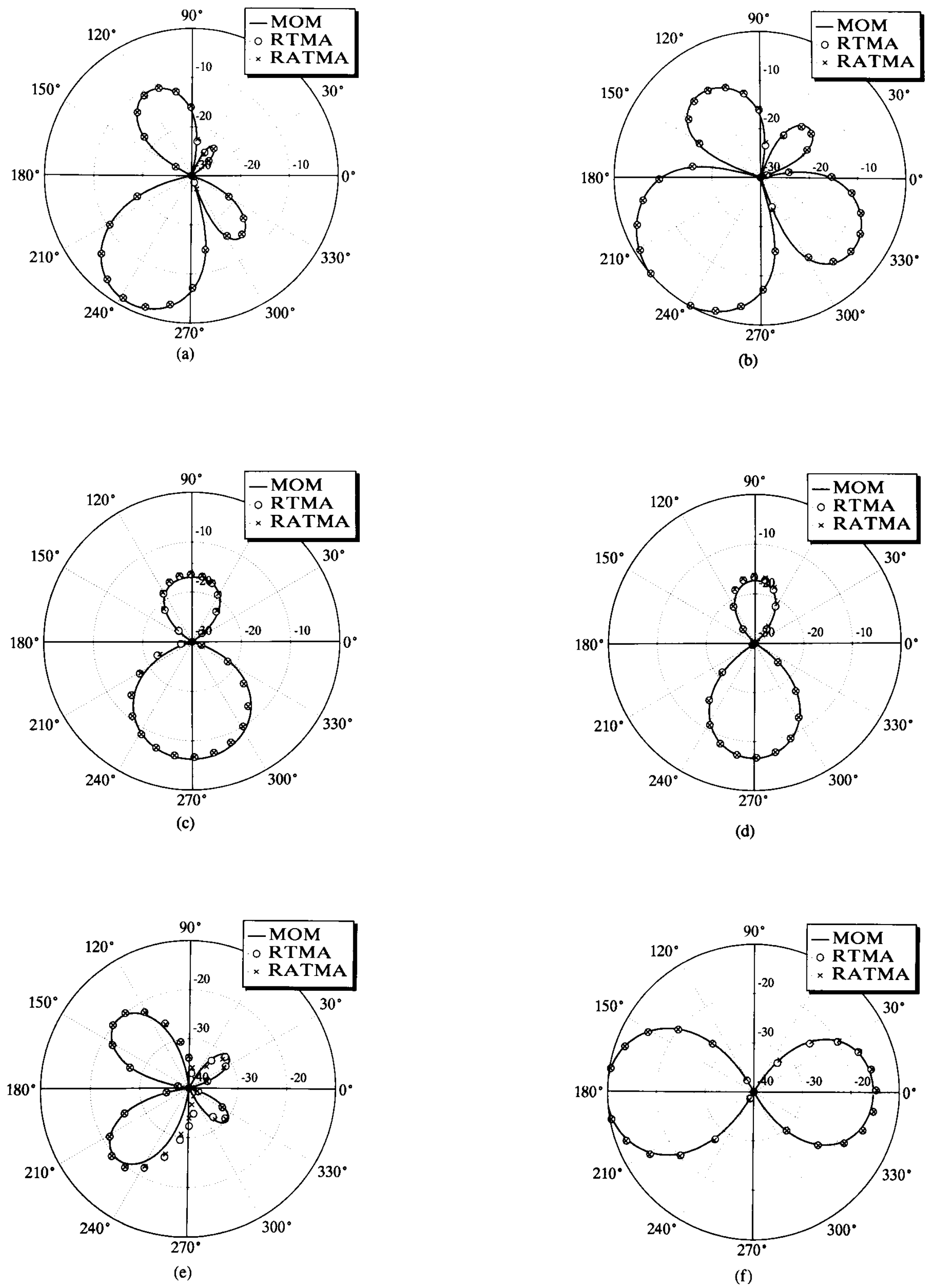

Fig. 4. RCS plots due to the 3 × 3 × 3 array configuration of three-dimensional clustering of patches as in Fig. 2(b): **(a)** TE case on the $\phi = 0$ cut, **(b)** TE case on the $\phi = \frac{\pi}{2}$ cut, **(c)** TE case on the $\theta = \frac{\pi}{2}$ cut, **(d)** TM case on the $\phi = 0$ cut, **(e)** TM case on the $\phi = \frac{\pi}{2}$ cut, **(f)** TM case on the $\theta = \frac{\pi}{2}$ cut.

terers [Fig. 2(b)].

Considering the three possible clustering schemes, one can easily determine how the largest dimension of the geometry depends on the number of scatterers:

$$d_{\max} \propto N \quad \text{for one-dimensional clustering,} \tag{11a}$$

$$d_{\max} \propto N^{1/2} \quad \text{for two-dimensional clustering,} \tag{11b}$$

$$d_{\max} \propto N^{1/3} \quad \text{for three-dimensional clustering.} \tag{11c}$$

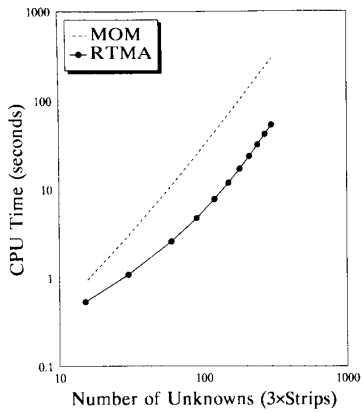

Fig. 5. Comparison of the CPU times required by the application of the MoM and the RTMA to the one-dimensional clusterings of strips as in Fig. 1(a).

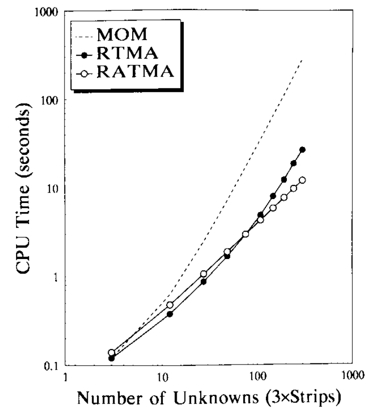

Fig. 6. Comparison of the CPU times required by the application of the MoM, the RTMA and the RATMA to the two-dimensional clusterings of strips as in Fig. 1(b).

Finally, (10) can be combined with (11) to determine the dependence of P on N

1) $P \propto N$ for one-dimensional clustering of two-dimensional scatterers,
2) $P \propto N^{1/2}$ for two-dimensional clustering of two-dimensional scatterers,
3) $\sqrt{P} \propto N^{1/2}$ for two-dimensional clustering of three-dimensional scatterers,
4) $\sqrt{P} \propto N^{1/3}$ for three-dimensional clustering of three-dimensional scatterers.

Tables I and II display the computational complexities and the memory requirements of both the RTMA and the RATMA for different clusterings of two-dimensional and three-dimensional scatterers. It is observed that $O(N^2)$ and $O(N^{7/3})$ computational complexities and $O(N)$ and $O(N^{4/3})$ memory requirements are possible for two-dimensional and three-dimensional scatterers, respectively. It is also observed that the denser the scatterers are clustered, the smaller the number of operations required by the RTMA's.

Note that the RTMA yields a full solution valid for all angles of incident waves. Comparisons with the performances of the conjugate-gradient algorithms that have reduced computational complexity will not be fair since they yield solutions valid for only one given incident wave.

V. Results

We have applied the RTMA's to the canonical strip and patch geometries of Figs. 1 and 2. Some of these geometries violate the restrictions [12] that are inherently imposed by the RTMA's presented in this paper; in that case, we have used one of the two techniques [8]–[10],[12] developed to lift these restrictions. In this section, we will present results for the two-dimensional and three-dimensional clusterings of patches. Results for the one-dimensional and two-dimensional clusterings of strips were given elsewhere [7]–[12].

Consider a plane wave, either TM or TE polarized, incident on an array of 7×7 conducting patches at $\phi = 0$ and $\theta = 45°$ as illustrated in Fig. 2(a). There are a total of 49 identical square patches with size $kw = 1.0$ and spacing $kd = 2.0$ in both the x and y directions. Fig. 3(a)–(f) show the normalized RCS plots (on a logarithmic scale) on the $\phi = 0$, $\phi = \frac{\pi}{2}$, and $\theta = \frac{\pi}{2}$ cuts, i.e., the x-z, y-z, and, x-y planes. Results obtained using the method of moments (MoM), the RTMA, and the RATMA for both the TE and TM cases are presented in these figures. Note that the three methods agree very well on all of the cuts and for both polarizations.

Next, consider a three-dimensional clustering of patches. We will investigate the $3 \times 3 \times 3$ patch geometry. A plane wave, either TM or TE polarized, is incident on the structure at $\phi = 0$ and $\theta = 45°$. The patches are identical and square in shape with size $kw = 1.0$ and spacing $kd = 2.0$ in all of the x, y, and z directions. The results presented in Fig. 4(a)–(f) for this 27-patch geometry also display good agreement between the MoM and the RTMA's.

VI. Performance of the RTMA's

A theoretical analysis of the computational complexities of the RTMA's was given earlier in this paper. Tables I and II display the complexities of the RTMA's when applied to two-dimensional and three-dimensional scatterers clustered in different dimensions. In this section, we will report the actual times that the computer programs based on the RTMA's take to run on a single central processing unit (CPU).

Figs. 5–8 display the CPU times taken by different computer programs based on the MoM, the RTMA, and the RATMA. In all of these figures, both the vertical and the horizontal axes are logarithmically scaled; therefore, the slope of a curve is equal to the order of the computational complexity of the corresponding algorithm.

Fig. 5 shows the CPU times taken by two programs based on the MoM and the RTMA when applied to the one-dimensional clusterings of strips [see Fig. 1(a)]. The slope of the RTMA is seen to be equal to that of MoM for large N (number of strips or number of unknowns). This observation agrees with the theoretical prediction of $O(N^3)$ computational complexity for the application of the RTMA to the one-dimensional clusterings of strips [see Table I, part (a)].

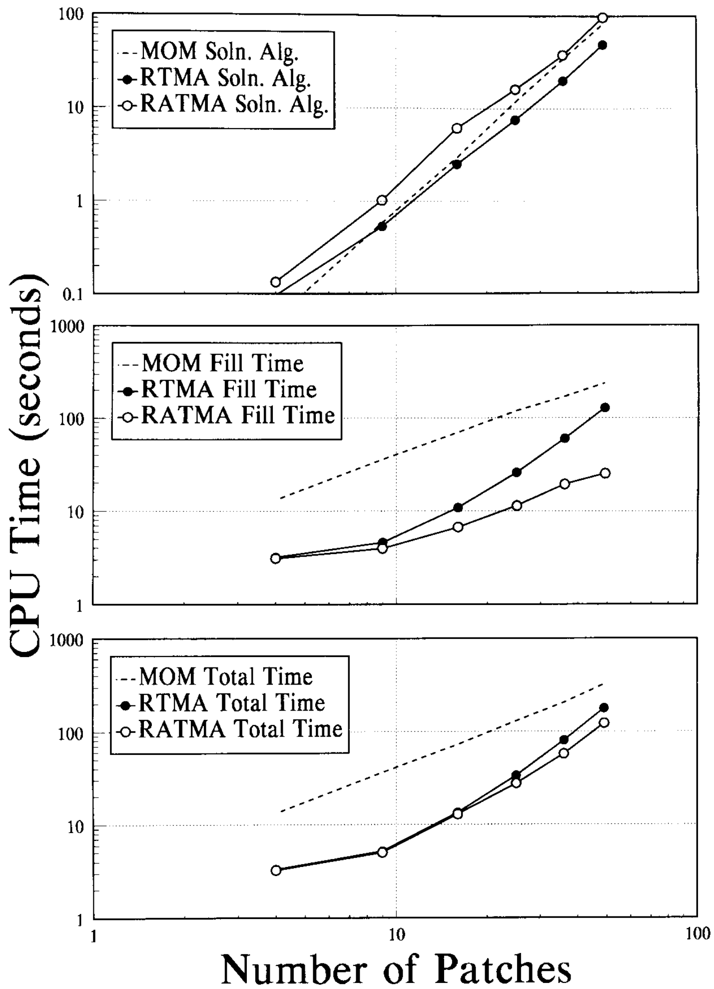

Fig. 7. Comparisons of the CPU times required by the applications of the MoM, the RTMA and the RATMA to the two-dimensional clusterings of patches as in Fig. 2(a).

Fig. 6 compares the CPU times taken by the MoM, the RTMA and the RATMA when applied to the two-dimensional clusterings of strips as in Fig. 1(b). It is observed that, for large N, the RATMA has the smallest slope, and the MoM has the largest slope. This finding also agrees with the theoretical predictions of Table I, part (a), in which the RTMA and the RATMA are shown to have $O(N^{5/2})$ and $O(N^2)$ computational complexities, respectively.

In Fig. 7, we present, in addition to the total CPU times taken by the MoM, the RTMA, and the RATMA when applied to the two-dimensional clusterings of patches [see Fig. 2(a)], the breakdown of the total CPU times into the matrix-filling times and actual matrix-solution times. The matrix-solution times for the MoM, the RTMA, and the RATMA have the same slopes for large N. This is in agreement with the predictions of Table II, part (a), where both the RTMA and the RATMA are shown to have $O(N^3)$ computational complexities, respectively.

Finally, in Fig. 8, we present the matrix-solution times, the matrix-fill times, and the total times required by the applications of the MoM, the RTMA, and the RATMA to the three-dimensional clustering of patches [see Fig. 2(b)]. We observe that, for large N, the RATMA has the smallest slope, whereas the MoM has the largest slope in the matrix-solution times. This finding agrees with the theoretical predictions of Table II, part (a), in which the RTMA and the RATMA are shown to have $O(N^{8/3})$ and $O(N^{7/3})$ computational complexities, respectively. The order of the slopes for the matrix-fill times is just the reverse, i.e., the RATMA has the largest slope, and the MoM has the smallest slope. However, for larger N, the matrix-solution time will be more dominant than the matrix-fill time. Indeed, Fig. 8 shows that the total CPU time of the RATMA is starting to be dominated by the matrix-solution time at the last data point ($N = 200$), whereas the total times of the MoM and RTMA are still dominated by the matrix-fill time.

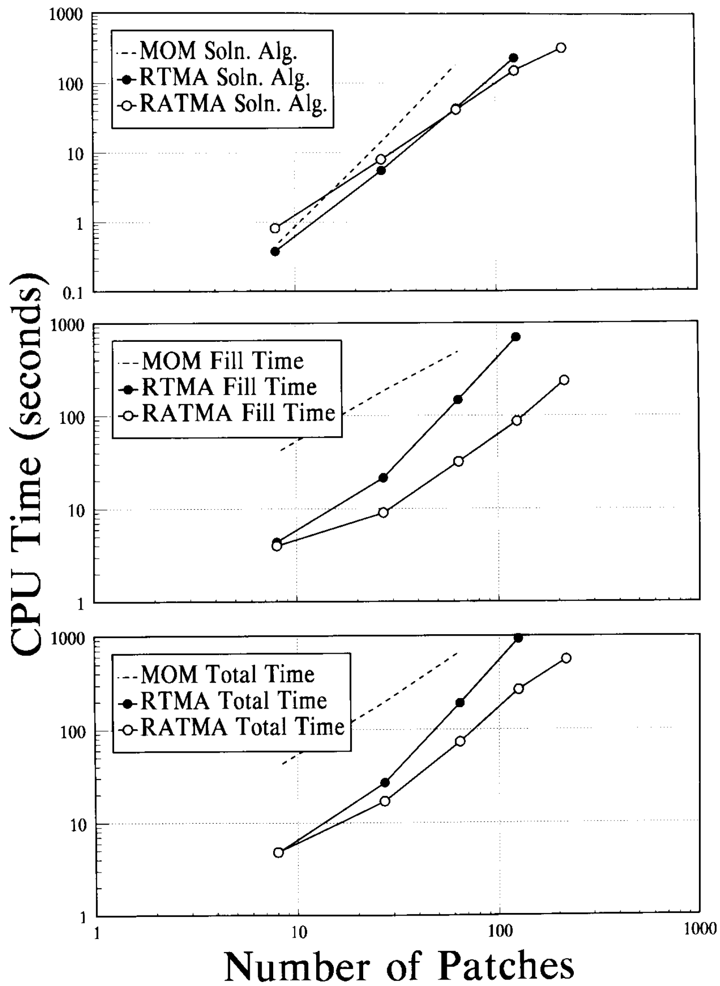

Fig. 8. Comparisons of the CPU times required by the applications of the MoM, the RTMA and the RATMA to the three-dimensional clusterings of patches as in Fig. 2(b).

VII. Conclusions

We have presented the applications of the RTMA and the RATMA to canonical strip and patch geometries. Computational complexities of $O(N^2)$ and $O(N^{7/3})$ and memory requirements of $O(N)$ and $O(N^{4/3})$ have been shown to be feasible for two-dimensional and three-dimensional geometries, respectively. We have applied these algorithms to electromagnetic scattering problems. They can also be extended to other wave-scattering problems, and even to problems in other disciplines. When solving the electromagnetic scattering problem, these algorithms give the full-wave solution without having to make any approximations on the fundamental equations and the boundary conditions. Being computational algorithms, they give the numerically approximate solution of the exact electromagnetic formulation. These algorithms also give the solution for all possible incident waves or "right-hand sides" at once, a feature that is not shared by some other fast solution techniques such as the conjugate-gradient method. Furthermore, as opposed to some other formulation schemes such as the finite-element method, these algorithms naturally incorporate the radiation condition at infinity; therefore, they can handle geometries in unbounded media. The formulation presented in this paper for patch problems uses scalar—instead of vector—addition theorems for spherical harmonic wave functions.

References

[1] W. C. Chew, "An N^2 algorithm for the multiple scattering solution of N scatterers," *Microwave Opt. Tech. Lett.*, vol. 2, pp. 380–383, Nov. 1989.

[2] W. C. Chew, J. A. Friedrich, and R. Geiger, "A multiple scattering solution for the effective permittivity of a sphere mixture," *IEEE Trans. Geosci. Remote Sensing*, vol. GE-28, pp. 207–214, Mar. 1990.

[3] Y. M. Wang and W. C. Chew, "An efficient algorithm for solution of a scattering problem," *Microwave Opt. Tech. Lett.*, vol. 3, pp. 102–106, Mar. 1990.

[4] W. C. Chew and Y. M. Wang, "A fast algorithm for solution of a scattering problem using a recursive aggregate $\overline{\tau}$ matrix method," *Microwave Opt. Tech. Lett.*, vol. 3, pp. 164–169, May 1990.

[5] W. C. Chew, *Waves and Fields in Inhomogeneous Media.* New York: Van Nostrand Reinhold, 1990.
[6] Y. M. Wang and W. C. Chew, "Application of the fast recursive algorithm to a large inhomogeneous scatterer for TM polarization," *Microwave Opt. Tech. Lett.*, vol. 4, pp. 155–157, Mar. 1991.
[7] L. Gürel and W. C. Chew, "A recursive T-matrix algorithm for strips and patches," *Radio Sci.*, vol. 27, pp. 387–401, May-June 1992.
[8] W. C. Chew, L. Gürel, Y. M. Wang, G. Otto, R. Wagner, and Q. H. Liu, "A generalized recursive algorithm for wave-scattering solutions in two dimensions," *IEEE Trans. Microwave Theory Tech.*, vol. MTT-40, pp. 716–723, Apr. 1992.
[9] W. C. Chew, Y. M. Wang, and L. Gürel, "Recursive algorithm for wave-scattering solutions using windowed addition theorems," *J. Electromagnetic Waves and Applications*, vol. 6, no. 11, pp. 1537–1560, 1992.
[10] W. C. Chew, Y. M. Wang, L. Gürel, and J. H. Lin, "Recursive algorithms to reduce the computational complexity of scattering problems," in *7th Annual Review of Progress in Applied Computational Electromagnetics, Conference Proceedings*, Monterey, CA, Mar. 1991, pp. 278–291.
[11] L. Gürel and W. C. Chew, "Recursive T-matrix algorithms for 1-D and 2-D clusterings of strips," in *1991 International IEEE/AP-S Symposium Digest*, London, Ontario, Canada, June 1991, pp. 276–279.
[12] L. Gürel, "Recursive algorithms for computational electromagnetics," Ph.D. dissertation, University of Illinois, Champaign-Urbana, IL, 1991.
[13] W. C. Chew, "Recurrence relations for three-dimensional scalar addition theorem," *J. Electromagnetic Waves and Applications*, vol. 6, no. 2, pp. 133–142, 1992.
[14] P. C. Waterman, "Matrix formulation of electromagnetic scattering," *Proc. IEEE*, vol. 53, pp. 805–812, Aug. 1965.
[15] R. H. T. Bates, "Modal expansions for electromagnetic scattering from perfectly conducting cylinders of arbitrary cross-section," *Proc. IEE*, vol. 115, pp. 1443–1445, Oct. 1968.
[16] P. C. Waterman, "Scattering by dielectric obtacles, presented at URSI Symposium on Electromagnetic Waves, Steresa, Italy, 24–29 June, 1969, published in *Alta Freq.*, vol. 38 (Speciale), 1969, pp. 348–352.
[17] ——, "New formulation of acoustic scattering," *J. Acous. Soc. Am.*, vol. 45, no. 6, pp. 1417–1429, 1969.
[18] ——, "Symmetry, unitarity, and geometry in electromagnetic scattering," *Phys. Rev. D*, vol. 3, pp. 825–839, Feb. 1971.
[19] V. K. Varadan and V. V. Varadan, Eds., *Acoustic, Electromagnetic and Elastic Wave Scattering–Focus on the T-Matrix Approach*, Elmsford, NY: Pergamon, 1980.
[20] B. Peterson and S. Ström, "T matrix for electromagnetic scattering from an arbitrary number of scatterers and representations of E(3)," *Phys. Rev. D*, vol. 8, pp. 3661–3678, Nov. 1973.
[21] ——, "Matrix formulation of acoustic scattering from an arbitrary number of scatterers," *J. Acous. Soc. Am.*, vol. 56, pp. 771–780, Sept. 1974.
[22] ——, "T-matrix formulation of electromagnetic scattering from multilayered scatterers," *Phys. Rev. D*, vol. 10, pp. 2670–2684, Oct. 1974.
[23] ——, "Matrix formulation of acoustic scattering from multilayered scatterers," *J. Acous. Soc. Am.*, vol. 57, pp. 2–13, Jan. 1975.
[24] D. S. Wang and P. W. Barber, "Scattering by inhomogeneous nonspherical objects," *Appl. Opt.*, vol. 18, pp. 1190–1197, Apr. 1979.
[25] P. C. Waterman, "Matrix methods in potential theory and electromagnetic scattering," *J. Appl. Phys.*, vol. 50, pp. 4550–4566, July. 1979.
[26] R. L. Weaver and Y. H. Pao, "Application of the transition matrix to a ribbon-shaped scatterer," *J. Acous. Soc. Am.*, vol. 66, pp. 1199–1206, Oct. 1979.
[27] P. M. van den Berg, "Transition matrix in acoustic scattering by a strip," *J. Acous. Soc. Am.*, vol. 70, pp. 615–619, Aug. 1981.
[28] G. Kristensson and P. C. Waterman, "The T matrix for acoustic and electromagnetic scattering by circular disks," *J. Acous. Soc. Am.*, vol. 72, pp. 1612–1625, Nov. 1982.
[29] S. Ström and W. Zheng, "Basic features of the null field method for dielectric scatterers," *Radio Sci.*, vol. 22, pp. 1273–1281, Dec. 1987.
[30] ——, "The null field method approach to electromagnetic scattering from composite objects," *IEEE Trans. Antennas Propagat.*, vol. AP-36, pp. 376–382, Mar. 1988.
[31] W. Zheng, "The null field to electromagnetic scattering from composite objects: The case with three or more constituents," *IEEE Trans. Antennas Propagat.*, vol. AP-36, pp. 1396–1400, Oct. 1988.
[32] S. Ström and W. Zheng, "The null field method approach to electromagnetic scattering from composite objects: The case of concavo-convex constituents," *IEEE Trans. Antennas Propagat.*, vol. AP-37, pp. 373–383, Mar. 1989.
[33] E. K. Miller, "A selective survey of computational electromagnetics," *IEEE Trans. Antennas Propagat.*, vol. AP-36, pp. 1281–1305, Sept. 1988.
[34] F. X. Canning, "Transformations that produce a sparse moment method matrix," *J. Electromagnetic Waves and Applications*, vol. 4, pp. 983–913, 1990.
[35] ——, "The impedance matrix localization (IML) method for moment-method calculations," *IEEE Antennas Propagat. Magazine*, vol. 32, pp. 18–30, Oct. 1990.
[36] V. Rokhlin, "Rapid solution of integral equations of classical potential theory," *J. Comput. Phys.*, vol. 60, pp. 187–207, Sept. 1985.
[37] L. Greengard and V. Rokhlin, "A fast algorithm for particle simulations," *J. Comput. Phys.*, vol. 73, pp. 325–348, 1987.
[38] J. Carrier, L. Greengard, and V. Rokhlin, "A fast adaptive multipole algorithm for particle simulations," *SIAM J. Sci. Stat. Comput.*, vol. 9, pp. 669–686, July 1988.
[39] V. Rokhlin, "Rapid solution of integral equations of scattering theory in two dimensions," *J. Comput. Phys.*, vol. 86, pp. 414–439, Feb. 1990.
[40] R. W. Hockney and J. W. Eastwood, *Computer Simulation Using Particles.* New York: McGraw Hill, 1981.
[41] O. Axelsson and V. A. Barker, *Finite Element Solution of Boundary Value Problems.* Orlando, FL: Academic Press, 1984.

Levent Gürel (S'87–M'92) was born in Izmir, Turkey, in 1964. He received the B.Sc. degree from the Middle East Technical University (METU), Ankara, Turkey, in 1986, and the M.S. and Ph.D. degrees from the University of Illinois at Urbana-Champaign in 1988 and 1991, respectively, all in electrical engineering.

He joined the Thomas J. Watson Research Center of the International Business Machines Corporation, Yorktown Heights, NY, in 1991, where he has been working on the electromagnetic problems related to electronic packaging using numerical and analytical techniques. Dr. Gürel is also interested in the theoretical and computational aspects of microwave cavity applications, electromagnetic compatibility and interference analyses, millimeter wave and microwave integrated circuits, and fast algorithms designed to solve the electromagnetic (scattering, radiation, resonance, guidance, etc.) problems of inhomogeneous and layered media, high-speed electronic circuits, and frequency-selective surfaces.

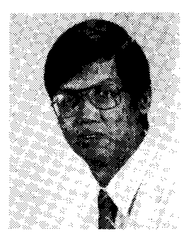

Weng Cho Chew (S'79–M'80–SM'86–F'93) was born on June 9, 1953 in Malaysia. He received the B.S. degree in 1976, the M.S. and Engineer's degrees in 1979, and the Ph.D. degree in 1980, all in electrical engineering from the Massachusetts Institute of Technology, Cambridge.

From 1981 to 1985, he was with Schlumberger-Doll Research in Ridgefield, CT. While there, he was a Program Leader and later a Department Manager. From 1985 to 1990, he was an Associate Professor with the University of Illinois, where he is currently a Professor. His research interests have been in the area of wave propagation and interaction with inhomogeneous media for geophysical subsurface sensing, nondestructive testing, microwave and millimeter wave integrated circuit, and microstrip antenna applications. He has also studied electrotechnical effects and dielectric properties of composite materials.

Dr. Chew is a member of Eta Kappa Nu, Tau Beta Pi, and URSI; and an active member of the Society of Exploration Geophysics. He is an NSF Presidential Young Investigator for 1986. He was an AdCom member and an Associate Editor with the IEEE TRANSACTIONS ON GEOSCIENCE AND REMOTE SENSING. He is also an Associate Editor with the *International Journal of Imaging Systems and Technology* and *Asia Pacific Engineering Journal*, and has been a Guest Editor with *Radio Science* and *International Journal of Imaging Systems and Technology*. In addition, he is an Associate Director of the Advanced Construction Technology Center at the University of Illinois.